THE JOURNAL OF BIOLOGICAL CHEMISTRY VOL. 287, NO. 29, pp. 24263–24272, July 13, 2012

Complex Cisplatin-Double Strand Break (DSB) Lesions Directly Impair Cellular Non-Homologous End-Joining (NHEJ) Independent of Downstream Damage Response (DDR) Pathways*[S]

Received for publication, January 21, 2012, and in revised form, May 18, 2012 Published, JBC Papers in Press, May 23, 2012, DOI 10.1074/jbc.M112.344911

Catherine R. Sears[‡] **and John J. Turchi**[‡§1]

From the [‡]*Departments of Medicine and* [§]*Biochemistry and Molecular Biology, Indiana University School of Medicine, Indianapolis, Indiana 46202*

Background: The biochemical mechanism of cisplatin-IR synergy is incompletely understood.
Results: NHEJ of non-cisplatin damaged DNA substrates is unaltered by cellular cisplatin treatment while repair of cisplatin-DSB lesions is inhibited independent of cellular cisplatin treatment.
Conclusion: Cisplatin-DSB compound lesions directly inhibit NHEJ while cisplatin-activated pathways do not impact NHEJ.
Significance: The mechanism of cisplatin-IR synergy involves direct inhibition of NHEJ by compound cisplatin-DSB lesions.

The treatment for advanced stage non-small cell lung cancer (NSCLC) often includes platinum-based chemotherapy and IR. Cisplatin and IR combination therapy display schedule and dose-dependent synergy, the mechanism of which is not completely understood. In a series of *in vitro* and cell culture assays in a NSCLC model, we investigated both the downstream and direct treatment and damage effects of cisplatin on NHEJ catalyzed repair of a DNA DSB. The results demonstrate that extracts prepared from cisplatin-treated cells are fully capable of NHEJ catalyzed repair of a DSB using a non-cisplatin-damaged DNA substrate *in vitro*. Similarly, using two different host cell reactivation assays, treatment of cells prior to transfection of a linear, undamaged reporter plasmid revealed no reduction in NHEJ compared with untreated cells. In contrast, transfection of a linear GFP-reporter plasmid containing site-specific, cisplatin lesions 6-bp from the termini revealed a significant impairment in DSB repair of the cisplatin-damaged DNA substrates in the absence of cellular treatment with cisplatin. Together, these data demonstrate that impaired NHEJ in combined cisplatin-IR treated cells is likely the result of a direct effect of cisplatin-DNA lesions near a DSB and that the indirect cellular effects of cisplatin treatment are not significant contributors to the synergistic cytotoxicity observed with combination cisplatin-IR treatment.

Lung cancer is the leading cause of cancer death in the United States, the majority of which are classified as non-small cell lung cancer (NSCLC).[2] Most of these are diagnosed at an advanced stage when surgical excision is often not an option (1–3). For these patients, first line therapy typically includes a platinum derivative, such as *cis*-diaminedichloroplatinum (II) (cisplatin), often used in combination with IR (4, 5). Cisplatin is a potent chemotherapeutic agent that has been used for decades to treat a variety of cancers, including testicular, ovarian, head and neck and lung cancer. Cisplatin directly interacts with multiple cellular components including proteins, thiol-containing peptides and nucleic acids (6). Cisplatin-DNA adducts are responsible for the majority of cisplatin cytotoxicity (7). Covalent binding of cisplatin to primarily purine bases of DNA results in mono-, inter-, and intra-strand adducts, causing distortion of the DNA double helix, which can block DNA replication and transcription (6). The more prevalent intra-strand cisplatin-DNA adducts are repaired by the nucleotide excision repair (NER) pathway and increased cisplatin toxicity is observed in NER-deficient cells. This effect is seen clinically in testicular cancer, which often presents with low expression of NER proteins, such as XPA and ERCC1, and displays exquisite sensitivity to cisplatin (8). Increased sensitivity to cisplatin has also been demonstrated in human NSCLC cells transfected with antisense XPA mRNA, highlighting the importance of NER in modulating cisplatin sensitivity (9). In addition to and as a result of cisplatin-induced DNA damage, many downstream effects develop following cisplatin treatment, including DNA-damage signaling responses, specifically impaired transcription, cell cycle arrest, and apoptosis (10–12). These downstream cellular responses caused by cisplatin treatment are central to the cytotoxic effects of cisplatin treatment on cancer cells.

IR treatment induces alterations in membrane proteins and lipids, impairment of protein function and increases in cell membrane permeability and, like cisplatin, its toxic effects are primarily attributed to the generation of DNA damage. IR damages DNA directly and indirectly through the formation of free

* This work was supported, in whole or in part, by National Institutes of Health Grant CA082741 (to J. J. T.).
[S] This article contains supplemental Figs. S1–S4 and methods.
[1] To whom correspondence should be addressed: Department of Medicine, Division of Hematology and Oncology, 980 W. Walnut Joseph E Walther Hall, R3 C650, Indianapolis, IN 46202. Tel.: 317-278-1996; Fax: 317-274-0396; E-mail: jturchi@iupui.edu.
[2] The abbreviations used are: NSCLC, non-small cell lung cancer; IR, ionizing radiation; DSB, double strand break; NHEJ, non-homologous end-joining; NER, nucleotide excision repair; DNA-PK, DNA-protein kinase; DNA-PKcs, DNA-protein kinase catalytic subunit; CFE, cell-free extract; HR, homologous recombination; RFP, red fluorescent protein; GFP, green fluorescent protein.

radical and reactive oxygen species, causing alterations in nucleotide bases, sugar fragmentation, formation of DNA-protein cross-links and generation of single and double strand DNA breaks. IR-induced DSBs are complex, often containing base overhangs, oxidative damage, and fragmented sugars, which present significant challenges for accurate repair. In humans, the NHEJ pathway is required for efficient repair of IR-induced DSBs and is considered error-prone (13). Following the formation of a DNA DSB, NHEJ is initiated when the Ku heterodimer binds to the DNA terminus and translocates down the length of the DNA, recruiting the DNA-PKcs, which together make up DNA-PK. After binding to DNA, DNA-PK is auto-phosphorylated and recruits and activates other proteins, including ligation factors and end-processing proteins (13).

While the role of NHEJ in the repair of IR-induced DSBs and radiation sensitivity is well established (14), the mechanism by which NHEJ contributes to cisplatin radiosensitization is less clear. Cisplatin has been shown to sensitize cancer cells to IR, both *in vitro* and *in vivo* (4, 15–17). We have demonstrated a synergistic interaction between cisplatin and IR in an ovarian cancer model (15). The synergistic interaction between cisplatin and IR is dependent on cisplatin concentration, IR dosage, and the duration and timing of treatment (15, 18). The increased cytotoxicity that is observed with cisplatin and IR treatment is temporal, requiring treatment with cisplatin prior to or concomitant to treatment with IR in both cell culture models (19, 20) and *in vivo* (21). The increased cytotoxicity seen with combined cisplatin and IR treatment is dependent on the NHEJ pathway, as DNA-PKcs-null cells, while hypersensitive to IR, do not display synergy with cisplatin (15). Increased sensitivity to combination cisplatin-IR treatment has also been observed in cells deficient in other proteins involved in IR-induced DSB repair (15, 18, 22). Global treatment of DNA with increasing concentrations of cisplatin has been investigated in an *in vitro* model and causes a decrease in DSB repair (23). *In vitro*, cisplatin adducts in close proximity to the DNA terminus inhibit DNA-PK activation, a necessary step in NHEJ (24, 25). Furthermore, we have previously demonstrated the presence of a site-specific cisplatin-DNA lesion near the terminus of a DSB completely abrogates DSB repair *in vitro* (15).

While the presence of complex DNA lesions consisting of a DNA DSB with a closely approximated cisplatin adduct has been demonstrated to impair DSB repair, if and how the downstream effects of cisplatin treatment impact repair of DNA DSBs has not been determined. In addition to its direct DNA interactions, cisplatin activates downstream DNA-damage signaling pathways causing activation of cell cycle checkpoints and ultimately can result in apoptosis (7, 10). Additionally, DSB repair of DNA containing cisplatin terminal lesions has never been directly investigated intracellularly. This manuscript explores the relationship between cisplatin treatment and DSB repair by separately evaluating the effects of cisplatin-DNA adduct formation and activation of downstream signaling pathways on NHEJ-dependent DSB repair in a NSCLC cell line. Data presented demonstrate that a cisplatin adduct in proximity to a DSB results in reduced NHEJ in the absence of cellular treatment with cisplatin. Furthermore, we demonstrate that the downstream cellular effects of cisplatin treatment have no appreciable impact on NHEJ catalyzed joining of a non-cisplatin-damaged DSB. These data support the hypothesis that the synergistic cell death observed with combined cisplatin-IR treatment is a function of a cisplatin-DNA lesion near the site of a DSB and independent of DNA damage signaling.

EXPERIMENTAL PROCEDURES

Materials

All reagents were purchased from Thermo Fisher Scientific (Waltham, MA), unless otherwise stated. All restriction enzymes were purchased from New England Biolabs (NEB, Beverly, MA) and carried out according to the manufacturer's instructions, with modifications as noted.

Cell-free Extract Preparation

CFEs were prepared according to previously published methods (27) with the following modifications. H460 cells were plated at 2×10^6 cells in eight 125-cm^2 flasks in complete RPMI medium and grown to 70–80% confluence. Cells were then mock treated or treated with 2 μM cisplatin for 3 h. Cisplatin containing media was removed, the cells washed three times with PBS, refed with complete media and incubated for 16 h at 37 °C. The cells were then harvested by trypsinization, washed with PBS, resuspended in 500 μl of the hypotonic buffer, and processed as previously described. Protein concentration was measured using a Bradford assay (Bio-Rad) according to the manufacturer's instructions, and the extracts were stored at −80 °C in buffer dialyzed against 25 mM HEPES-KOH, 100 mM KCl, 12 mM $MgCl_2$, 1 mM EDTA, 2 mM DTT, and 20% glycerol.

In Vitro NHEJ Assay

In vitro NHEJ assays were performed as previously published (15, 28) with the following modifications. Cell-free extracts (20 μg) were incubated with NU7441 or DMSO (2%) at the indicated concentrations for 10 min at 37 °C prior to the addition of ^{32}P-labeled DNA (10 ng, EcoR1-linearized pCAG-GFP). The DNA products were either analyzed by direct electrophoresis on a 0.6% agarose gel or following digestion with HinP1I, analyzed by 6% native PAGE. Following electrophoresis the gels were dried and radioactivity quantified by PhosphorImager analysis using ImageQuant software. Mann-Whitney Rank Sum analysis was used to determine statistical significance from duplicate determinations using both methodologies for product analysis.

Cell Culture and Drug Treatment

H460 cells were grown in RPMI supplemented with L-glutamine, penicillin/streptomycin and 10% fetal bovine serum (Atlanta Biologicals). A549 cells were grown in DMEM (Dulbecco's modified Eagle's medium) supplemented with 4.5 g/liter glucose and L-glutamine, 1% penicillin/streptomycin, and 10% fetal bovine serum. Cells were incubated at 37 °C in a humidified 5% CO_2 atmosphere. Cisplatin (Sigma) was added at the indicated concentrations to the complete medium and incubations occurred for 3 h at 37 °C. Following incubation, the cells were washed three times with PBS before further processing. NU7441 was stored at 5 mM in DMSO. For experiments

using NU7441, H460 cells were incubated with DMSO (0.2%) or NU7441 (1 or 10 μM) for 1 h prior to transfection and following transfection for the duration of the experiment.

Preparation of Cisplatin-damaged NHEJ Substrate

To create a plasmid substrate with terminal cisplatin lesions, 30 bp linkers containing a site-specific 1,2d (GpG) cisplatin lesion 6 bp from the terminus were ligated to the linearized plasmid (supplemental Fig. S1*A*) (15). Briefly, the pGL-1-Mfe1 plasmid (see supplemental methods) was linearized with AvrII in an overnight digestion at 37 °C. The oligonucleotide SJC1.5 was treated with cisplatin in a 1:3 molar ratio and the cisplatin adducted substrate was purified by preparative 12% denaturing PAGE (26). The oligonucleotide SJC1.5C-*Xba* was 5′ phosphorylated using T4 polynucleotide kinase and annealed to platinated or control SJC 1.5 in a 1:2 molar ratio, forming the cisplatin damaged and undamaged duplex linkers. The control and cisplatin damaged duplex oligonucleotides were mixed with AvrII-digested pGL1-Mfe1 in a 2:1 molar ratio, ethanol precipitated, and resuspended in 1× Ligase Buffer (New England Biolabs) containing T4 DNA ligase, AvrII, and XbaI, and ligation reactions preceded for 16 h at 18 °C as previously described (15). The addition of AvrII linearizes any pGL1-Mfe1 that might re-ligate without the linkers and the Xba1 reverses any linker-linker ligation. The plasmid-linker ligation events are not digested by either AvrII or XbaI. Complete ligation was confirmed by 5′ labeling with [γ-^{32}P]ATP using T4 polynucleotide kinase in 1× Exchange Reaction Buffer, then enzymatic digestion with SacI and separation of digestion products by 8% native PAGE (see supplemental Fig. S1, *B* and *C*).

Host Cell Reactivation Assays

Fluorescence Microscopy—For evaluation of NHEJ-dependent repair of compound cisplatin-DSB lesions, the prepared platinated and undamaged linear plasmids as described above were used. To investigate the downstream effects of cisplatin treatment on undamaged DNA, pCAG-GFP was used in a host cell reactivation assay. pCAG-GFP was linearized by restriction enzyme digestion with EcoR1, under the recommended conditions, and complete digestion was confirmed by agarose gel electrophoresis. Covalently closed circular pCAG-dsRED was used as a transfection control in all experiments.

For experiments investigating the downstream effects of cisplatin on NHEJ-dependent repair of undamaged DNA, H460, and A549 cells were plated at 5×10^4 cells/cm^2 in a 6-well plate and 24 h later were mock treated or treated with cisplatin as described above immediately prior to transfection. Cells were trypsinized and transfected with the indicated plasmids (2 μg) by electroporation using an Amaxa nucleofector device (Lonza, Basal, Switzerland) in medium from the cell line nucleofector kit T according to the manufacturer's instructions. After transfection, the cells were resuspended, placed in individual wells of a 6-well dish, and incubated in complete media at 37 °C for 48 h. The media was supplemented with DMSO or NU7441 in individual experiments at the indicated concentrations. Fluorescence microscopy was used to detect reporter activity, and images were captured using a Zeiss Axiovert microscope equipped with a digital camera (Axiovert 200 M, Zeiss, München-Hallbergmoos). To quantify the number of fluorescent cells, four images from each well were captured using MR Grab 1.0 (Zeiss) using filters for Texas Red (RFP) and FITC (GFP). Images were visualized and quantified using Image J software (NIH, Bethesda, MD). Relative GFP expression was determined by dividing then number of GFP expressing cells by the number of RFP expressing cells. NHEJ efficiency (percent efficiency) was calculated by dividing the relative GFP expression in cells transfected with linear pCAG-GFP to the relative GFP expression in cells transfected with circular pCAG-GFP. NHEJ efficiency was determined from individual experiments and standard deviations reported. For cisplatin- and NU7441-treated models, statistical analysis for significance was performed by paired *t* tests. Paired *t* test was used to determine significance between the relative GFP expressions in cells transfected with the platinated and undamaged plasmids.

For high magnification images, H460 cells were transfected as above and plated on cover slips (Corning, Corning, NY). After incubation for 48 h, cells were washed with PBS, fixed with 4% paraformaldehyde at room temperature for 8 min, counterstained with DAPI (300 nM) and washed again. The cover slips were inversely mounted and images were captured using a Zeiss fluorescent microscope using filters for DAPI, Texas Red, and FITC, and then analyzed using ImageJ software.

Dual Luciferase Assay—Investigation of the downstream effects of cisplatin treatment on undamaged DNA was performed by a dual luciferase assay. 24 h before treatment, A549 cells were plated at 1×10^4 cells/well in white, opaque 96-well plates (BD Falcon). Cells were treated with cisplatin or mock-treated as above. After 3 h, cells were washed twice with PBS and the media replaced with DMEM supplemented with FBS. Cells were transfected with either circular or HindIII-linearized pGL3-luc (100 ng) and the control vector pRL-TK (10 ng) using Fugene HD (Promega) according to the manufacturer's instructions. 24 h later, transfected cells were lysed and the luciferase activity (firefly and *Renilla*) were measured as relative light units (RLUs) using the Dual-Luciferase Reporter Assay System (Promega) in a luminometer (BioTek Synergy H1 Hybrid, Winooski, VT) according to the manufacturer's instructions. Relative luciferase activity was determined by dividing the firefly luciferase RLUs by the *Renilla* RLUs. Relative luciferase activities for each experimental condition were compared by Grubbs statistical analysis for statistical outliers using a two-tailed $\alpha<0.05$. Individual experiments were performed at least in triplicate. The average relative luciferase activity in cells transfected with the linear pGL3-luc plasmid were divided by the average relative luciferase activity in cells transfected with the circular pGL3-luc plasmid for each condition, and the means from three independent experiments and SDs are reported. Determination of statistical significance was by paired Student's *t* test.

Flow Cytometry

H460 cells were analyzed for apoptosis by an Alexa Fluor 480 Annexin V/Dead Cell Apoptosis Kit (Invitrogen) according to the manufacturer's instructions. Cells were plated 24 h prior to cisplatin treatment at 2.5×10^4 cells/cm^2 as described above. At the indicated time points, adherent and non-adherent cells

were collected and analyzed on a BD FACScan flow cytometer. Data were analyzed using WinMDI software (Scripps Research Institute, San Diego, CA). Cell cycle analysis was performed by propidium iodide staining. Briefly, adherent and non-adherent cells were collected at the indicated time points, washed with PBS containing 2% bovine serum albumin, resuspended in 70% cold ethanol and incubated at −20 °C for 24–48 h. Cells were collected and incubated in the dark with RNase A (25 μg/ml) and PI stain (1 μg/ml) for 30 min at 37 °C followed by 1.5 h at 4 °C. Flow cytometric analysis was performed on a BD FACScan and cell cycle distribution was analyzed using ModFit LT software (Verity Software House, Topsham, ME) with gated events plotted against the FL2-area parameter. Paired Student's *t* test was used to determine statistical significance.

DNA-PK Kinase Assays

Kinase assays were performed using Promega SignaTECT DNA-dependent Protein Kinase Assay System (Promega, Madison, WI) according to the manufacturer's instructions with the following modifications. Where indicated, NU7441 (Tocris Bioscience, Ellisville, MO) was incubated with the H460 cell-free extract (30 μg) at the indicated concentrations for 2 min before initiation and throughout the reaction. Quantification was performed by PhosphorImager analysis.

RESULTS

CFEs Prepared from Cisplatin-treated NSCLC Cells Support NHEJ Catalyzed Repair of a DNA DSB—We and others (15, 18, 19, 21) have shown that an intact NHEJ pathway is necessary for the synergy of cisplatin-IR combination therapy. We also have demonstrated that a CFE prepared from untreated cancer cells is capable of catalyzing NHEJ and that the presence of cisplatin lesions 6 bp from the termini of the DNA being rejoined are highly inhibitory (15). This result, however, does not rule out the possibility that NHEJ can also be indirectly influenced by cisplatin treatment and activation of the DNA damage response pathway. To assess this impact of cisplatin-activated downstream damage response pathways on NHEJ, we assessed *in vitro* NHEJ activity catalyzed by CFEs prepared from cisplatin treated and control extracts. The assay is schematically depicted in supplemental Fig. S2*A* along with data demonstrating that both plasmid rejoining and DNA-PK phosphorylation activity are inhibited by the DNA-PKcs inhibitor NU7441 (supplemental Fig. S2, *B–D*). These data indicate that our *in vitro* NHEJ plasmid rejoining assay is a measure of *bona fide* DNA-PKcs-dependent NHEJ-catalyzed DSB repair.

To determine if CFEs prepared from cisplatin-treated cells are capable of supporting NHEJ, H460 cells were either mock treated or treated with 2 μM cisplatin for 3 h. Following treatment, cells were incubated for an additional 16 h to allow for initiation of cellular DNA damage response processes after which CFEs were prepared. This concentration and duration of cisplatin treatment produced the expected cell cycle delay and eventual induction of apoptosis observed between 24 and 48 h post-treatment (supplemental Fig. S3). Thus, harvesting cells at 16 h post-treatment enabled us to recapitulate the cellular signaling processes prior to caspase activation and DNA-PKcs degradation (10). A direct comparison of NHEJ activity in CFE prepared from mock- and cisplatin-treated cells is presented in Fig. 1. Direct analysis of the joined products is presented in Fig. 1*A*, with formation of multimers of the 5.5 kbp plasmid observed over time. Joined products are also observed in reactions catalyzed by CFEs prepared from both the cisplatin treated and untreated cells. Quantification of the data is presented in *panel B* and demonstrates an increase in joining activity over time and similar levels of ligation between the treated and untreated cells.

To further confirm the nature of the products, a post-joining digestion step was performed using HinP1I, which generates different sized products dependent on the orientation of the ligation events (supplemental Fig. S2*A*). The results are presented in Fig. 1*C* and again demonstrate the formation of ligated products independent of cisplatin treatment with no observable change in distribution of the ligation events. Quantification of the data presented in *panel D* also demonstrates no significant difference in the efficiency of joining as a function of cisplatin treatment of the cells prior to extract preparation. These data demonstrate that cisplatin treatment of cells does not inhibit NHEJ-catalyzed repair of a non-platinum-damaged DNA *in vitro*.

NHEJ Host Cell Reactivation Assay—While our *in vitro* assays suggest that cisplatin treatment does not impair NHEJ catalyzed joining of a non-cisplatin damaged DNA substrate, we cannot eliminate the possibility that in intact cells, cellular events not accurately recapitulated using CFEs could differentially influence NHEJ. Therefore, we employed a host cell reactivation assay using a linearized plasmid in which the GFP reporter gene is separated from the promoter, thus, only after rejoining the plasmid is the promoter positioned to drive GFP gene expression. To avoid cisplatin adduct formation on the DNA being rejoined, we introduced the NHEJ substrates into the cells via electroporation following treatment of the cells with cisplatin. This assay methodology is depicted in supplemental Fig. S4 and ensures that the DNA to be rejoined via NHEJ is not subject to the damage by cisplatin, yet ensures that the cells develop cisplatin chromosomal DNA damage leading to induction of the requisite downstream events in the damage response pathway. As synergy between cisplatin and IR is observed with concurrent treatment (15, 18), we minimized the time between cisplatin treatment and electroporation, processing for electroporation immediately after removing cisplatin from the cells. To control for differences in transfection efficiency, all experiments involved co-transfection with circular pCAG-dsRED, which produces a RFP independent of NHEJ. In preliminary experiments it was determined that 24 and 48 h post-transfection was optimal for quantification via fluorescence microscopy (data not shown). To confirm that the end joining and hence reporter expression represents NHEJ activity, we again employed the DNA-PK inhibitor NU7441. The results presented in Fig. 2*A* are representative images of fields captured with each filter set and pseudo-colored for presentation. The top row of panels shows results from co-transfection of circular pCAG-GFP and circular pCAG-dsRED plasmid while the bottom row are images from cells co-transfected with linearized pCAG-GFP and circular pCAG-dsRED. The results demonstrate that GFP expression is detected in cells trans-

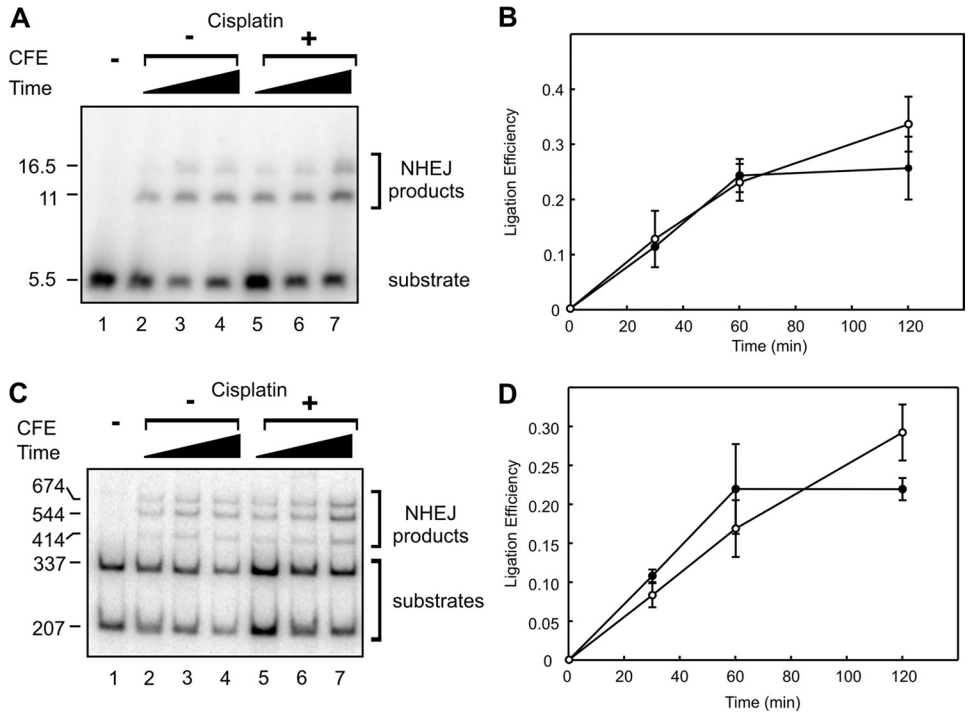

FIGURE 1. ***In vitro* NHEJ catalyzed by H460 extracts prepared from cisplatin treated cells.** *A*, NHEJ reactions were performed using 5′- ^{32}P end-labeled EcoR1-linearized pCAG-GFP and CFE from untreated (*lanes 2–4*) or cisplatin-treated (*lanes 5–7*) H460 cells. Reactions were terminated at 30, 60, and 120 min. NHEJ-dependent ligation products were directly resolved by 0.6% agarose gel electrophoresis. The position of the 5.5 kbp substrates is indicated along with the NHEJ ligation products at 11 and 16.5 kbp. *B*, quantification of the data presented in *panel A* along with an additional replicate. The mean and range of values are presented. Reactions performed with control CFEs are indicated by the *filled circles*, and cisplatin-treated CFEs by the *open circles*. *C*, following digestion by HinP1I, products were resolved by 6% native PAGE. Unligated head and tail products (207 and 337 bp) are seen along with ligated head-to-head, head-to-tail and tail-to-tail products (NHEJ products; 414, 544, and 674 bp, respectively). *D*, quantification of the data presented in *panel C* and an additional replicate. The mean and range of values are presented. Reactions performed with control CFEs are indicated by the *filled circles* and cisplatin-treated CFEs by the *open circles*. Using both methods of quantification, *in vitro* ligation efficiencies of CFEs from cisplatin-treated H460 cells at 30, 60, and 120 min do not significantly differ when compared with untreated controls ($p \geq 0.33$).

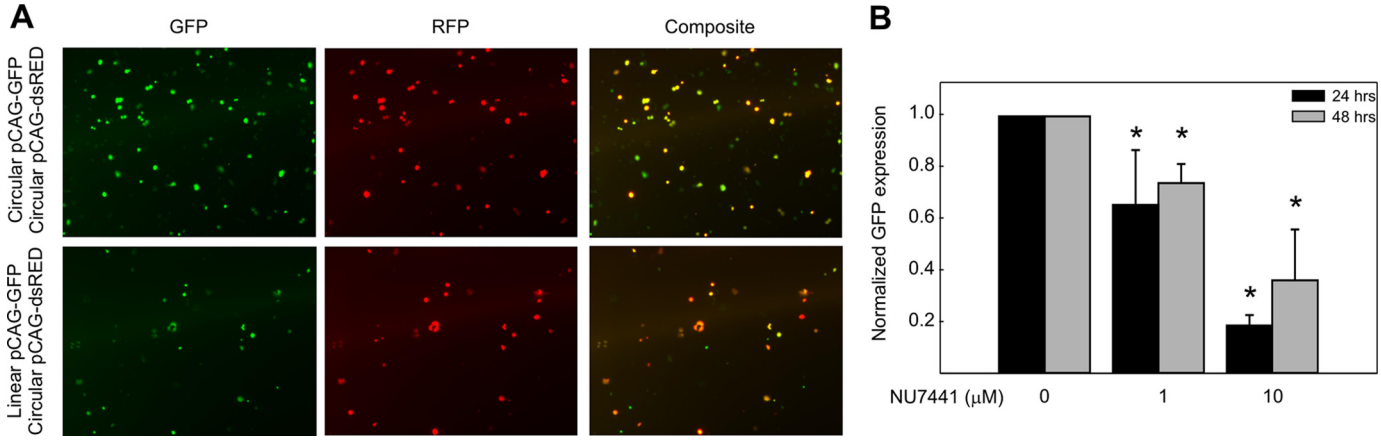

FIGURE 2. **Host cell reactivation assay for cellular NHEJ in H460 NSCLC cells.** *A*, H460 cells were treated with NU7441 (0, 1, 10 μM) for 1 h prior to transfection with either circular or EcoR1-linearized pCAG-GFP. Following transfection, cells are re-treated with NU7441 for an additional 24 or 48 h after which fluorescence microscopy images were collected at 80× magnification using the indicated filter set. The images were pseudo colored and overlaid by NIH Image J software. The images presented are from mock-treated controls. *B*, fluorescence data were quantified as described in "Experimental Procedures." Normalized GFP expression represents the number of GFP/RFP-positive cells from cells transfected with the linear GFP construct and circular RFP construct and normalized to the untreated control. Results from both 24 and 48 h are presented. The results are statistically significant when compared with untreated control (*, $p < 0.05$).

fected with the linear plasmid, indicative of NHEJ catalyzed rejoining. The number of cells expressing GFP and RFP were determined from four representative fields in three independent experiments and the results revealed that NHEJ catalyzed rejoining was consistently greater than 40% using the circular GFP as a reference. To demonstrate that the rejoining was in fact a DNA-PK dependent NHEJ event, sensitivity to NU7441 was investigated and the results from both 24 and 48 h post-transfection are presented in Fig. 2*B*. The values presented are the ratio of GFP/RFP-positive cells normalized to the vehicle-treated control. These results demonstrate sensitivity of the joining reaction to DNA-PK inhibition and support the conclusion that NHEJ is responsible for the observed DSB repair in this host cell reactivation assay.

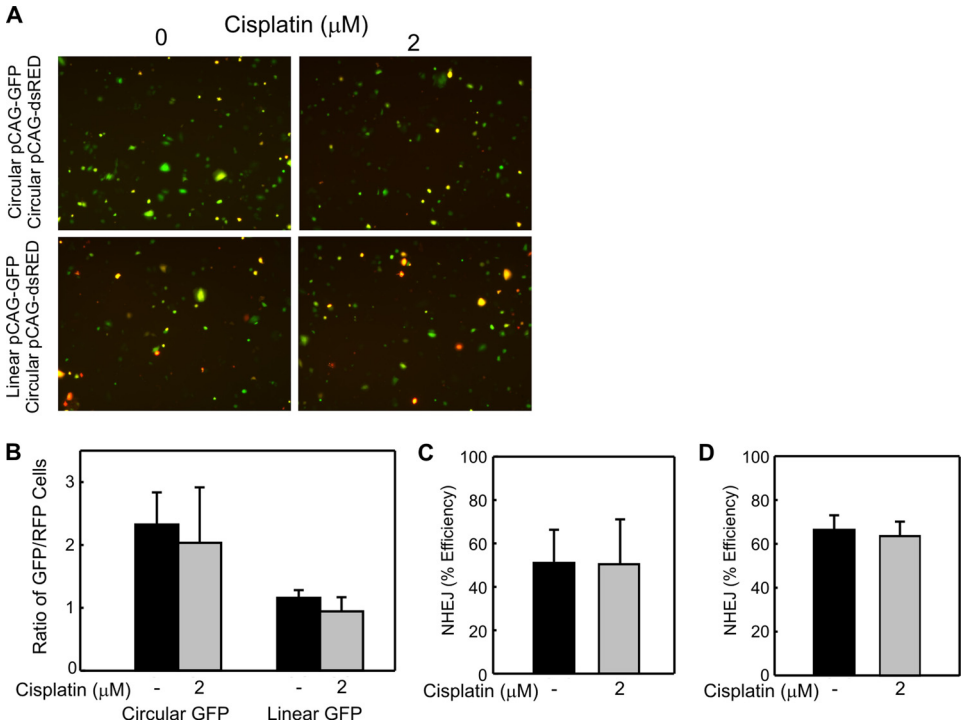

FIGURE 3. **Effect of cellular cisplatin treatment on NHEJ activity of an undamaged DNA in H460 NSCLC large cell carcinoma cells.** *A*, H460 cells were mock or cisplatin-treated as indicated and the indicated plasmid constructs transfected into cells immediately following cisplatin treatment as described under "Experimental Procedures." Fluorescence images were collected and processed as described in the legend to Fig. 2, with composite images shown. *B*, quantification of the relative GFP expression from three independent experiments was performed as described in "Experimental Procedures." The averages and S.D. are presented, and no statistically significant differences were observed as a function of cisplatin treatment. *C*, NHEJ efficiency in H460 cells was calculated by the relative GFP expression in cells transfected with linear pCAG-GFP divided by the relative GFP expression in cells transfected with circular pCAG-GFP. The means of three independent experiments and SDs are shown, and no statistically significant differences were observed following cisplatin treatment. *D*, H460 cells were mock or cisplatin treated as indicated followed by delayed transfection of plasmid constructs into cells 24 h after cisplatin treatment. NHEJ efficiency was calculated as above, and the means of two independent experiments performed in duplicate and variations from the mean are presented, showing no difference in NHEJ efficiency.

Cisplatin Treatment Does Not Impact NHEJ Activity of a Non-cisplatin-damaged DNA in Live Cells—To assess the impact of cisplatin on NHEJ in a cell culture model, cells were either mock treated or treated with 2 μM cisplatin for 3 h. At the end of 3 h, the cells were washed, harvested by trypsinization, and co-transfected with circular pCAG-dsRED and either linear or circular pCAG-GFP. Fluorescent images were captured 48 h following transfection and the composites are presented in Fig. 3*A*. The presence of GFP positive cells in the control samples transfected with circular pCAG-GFP indicates that cisplatin treatment does not alter the transcription and translation of GFP or RFP reporters (Fig. 3, *A* and *B*). The analysis of linear pCAG-GFP also revealed GFP positive cells, indicating that cellular cisplatin treatment does not abrogate NHEJ (Fig. 3*A*). Quantification of the data demonstrates that there is no significant difference in the relative GFP expression between the untreated and cisplatin treated cells transfected with circular pCAG-GFP and similarly, there was no significant difference in GFP expression between the untreated and cisplatin-treated H460 cells transfected with the EcoR1-linearized pCAG-GFP (Fig. 3, *B* and *C*). To ensure cisplatin-induced activation of downstream damage response pathways before measurement of *in situ* NHEJ activity, H460 cells were treated with cisplatin or mock treated as above, then allowed to incubate in drug-free media for 16 or 24 h before transfection of the reporter plasmids. No significant difference in NHEJ efficiency was observed following transfection delayed 24 (Fig. 3*D*) and 16 (data not shown) hours following cisplatin treatment. These data convincingly demonstrate that cisplatin-induced downstream cellular effects do not inhibit NHEJ activity.

To ensure that this finding is not unique to H460 cells, a similar series of experiments were repeated in the A549 NSCLC adenocarcinoma cell line. A549 cells were either mock treated or incubated with cisplatin at 2 and 4 μM for 3 h prior to co-transfection with circular pCAG-dsRED and either circular or linear pCAG-GFP. Representative fields are presented in Fig. 4*A*. Although transfection efficiency was decreased in this cell line as compared with H460 cells, evaluation for GFP and RFP expression at 48 h clearly revealed GFP expression in both cisplatin-treated groups following transfection of the linear GFP, and quantification revealed no significant difference in NHEJ efficiency observed between the untreated and cisplatin treated cells (Fig. 4, *B* and *C*), confirming that NHEJ-dependent repair of DSBs is independent of the downstream effects of cisplatin in a second NSCLC cell line.

To further confirm these findings, we utilized a similar methodology to investigate the impact of cisplatin-activated downstream damage response pathways on NHEJ using a dual luciferase assay. A549 cells were either mock treated or treated with 2 μM cisplatin for 3 h. At the end of 3 h, the cells were washed and co-transfected with circular pRL-TK and either linear or circular pGL3-luc. The relative light units (RLUs) for firefly and

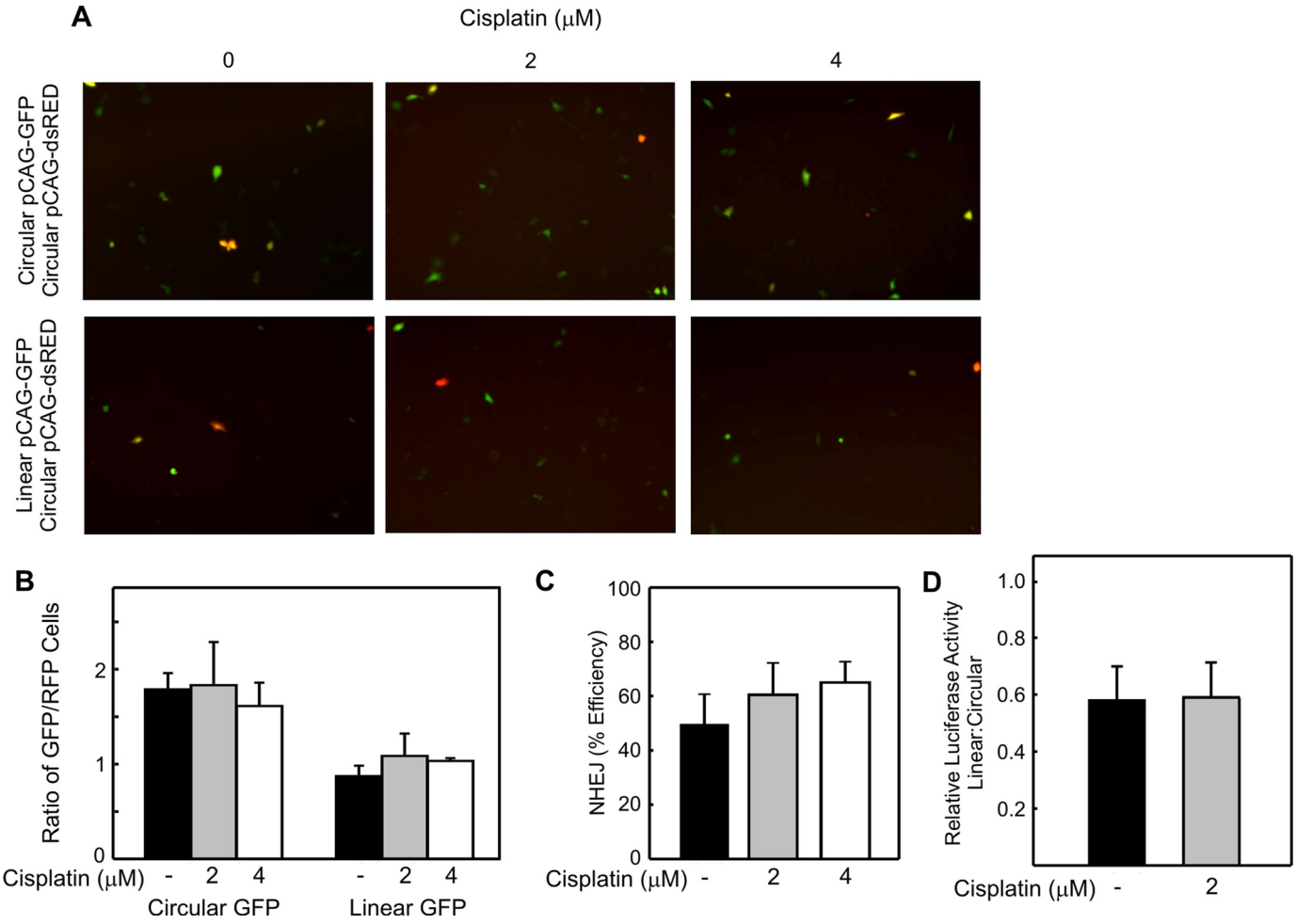

FIGURE 4. **Effect of cellular cisplatin treatment on NHEJ activity of an undamaged DNA in A549 NSCLC adenocarcinoma cells.** Cells were treated with the indicated concentration of cisplatin and transfected with the indicated DNA reporter constructs. *A*, fluorescence images were collected and processed as described in the legend to Fig. 2. *B*, fluorescence microscopy was quantified as described in "Experimental Procedures." The averages of three independent experiments and S.D. are presented, and no statistically significant differences were observed following cisplatin treatment at 2 and 4 μM. *C*, NHEJ efficiency in A549 cells was calculated by dividing the relative GFP expression in cells transfected with linear pCAG-GFP by the relative GFP expression in cells transfected with circular pCAG-GFP. The means of three independent experiments and SDs are presented, and no statistically significant differences in NHEJ efficiency were observed in either cisplatin-treated group when compared with control. *D*, following mock or cisplatin treatment, A549 cells were transfected with circular pRL-TK (transfection control) and either circular or linearized pGL3-luc. Relative luciferase activity was determined for each transfection by dividing firefly relative light units (RLUs) by *Renilla* RLUs. Ligation efficiency is represented by dividing the relative luciferase activity of the linear pGL3-luc transfected by the relative luciferase activity of the circular pGL3-luc transfected. The averages of three independent experiments and SD are presented, showing no statistically significant difference in relative ligation efficiency.

Renilla luciferase were measured at 24 h following transfection. Relative luciferase activity was determined by dividing the RLUs from the firefly luciferase by the RLUs from *Renilla* luciferase for each transfection. *In situ* ligation efficiency was determined by dividing the relative luciferase activity of the linear pGL3-luc transfected cells by the relative luciferase activity of the circular pGL3-luc-transfected cells and are presented in Fig. 4*D*. The results show no statistically significant difference in the ligation efficiency of unaltered DNA by cisplatin-induced activation of downstream damage response pathways.

Taken together, these data show that NHEJ-dependent repair of non-platinated DNA is preserved in cultured NSCLC cells treated with cisplatin, indicating that downstream activation of damage response pathways caused by cisplatin treatment has no significant effect on NHEJ-dependent DSB repair.

DNA-Cisplatin End-lesions Reduce NHEJ Activity in a Cell Culture Model—Our previous work demonstrated that *in vitro* NHEJ catalyzed repair of a substrate could be completely blocked by the presence of terminal cisplatin adducts (15). This result was consistent with our earlier research demonstrating that cisplatin-DNA damage inhibits DNA-PKcs activity (24, 29), a requisite step in NHEJ-dependent DSB repair and was also consistent with the proposed mechanism of cisplatin-IR synergy involving compound DNA damage with a cisplatin lesion in close proximity to the DSB. Data thus far suggest that activation of the downstream damage response pathways by cisplatin does not impact NHEJ, leaving the possibility that the abrogation of joining by cisplatin is completely a function of the direct effect of cisplatin lesions near the terminus of the DNA being rejoined. Therefore, we constructed a NHEJ substrate containing site-specific cisplatin lesions 6 base-pairs from each termini of a linearized plasmid. Again, the DSB was positioned between the CMV promoter and GFP structural gene, ensuring that GFP expression would only be detected with ligation of the plasmid (supplemental Fig. S1*A*). Stringent evaluations post-modification of the plasmid ensured near-complete platination

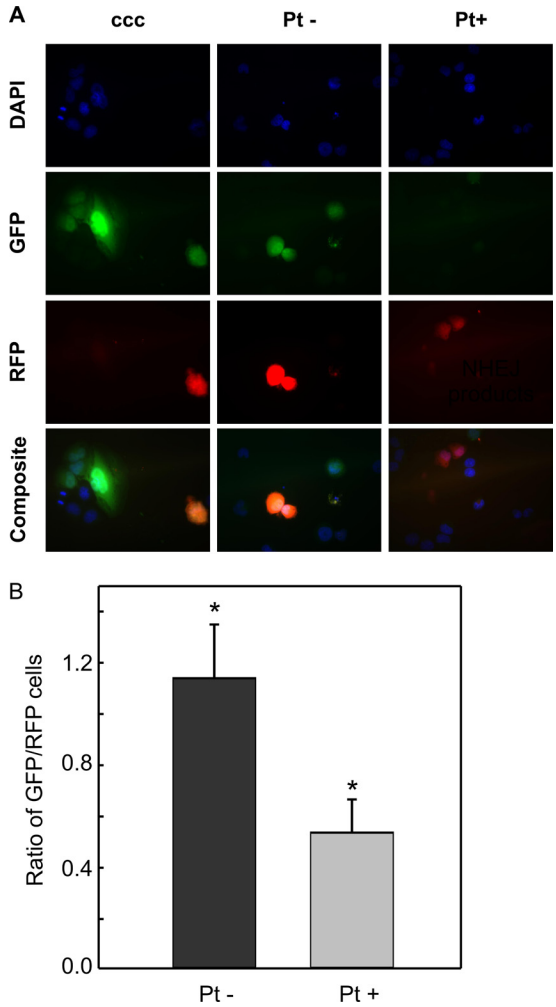

FIGURE 5. **Effect of cisplatin-DNA end-lesions on NHEJ activity in untreated H460 cells.** *A*, H460 cells were transfected with the indicated reporter constructed plasmids and incubated for 48 h. After fixing on a coverslip, cells were counterstained with DAPI and evaluated for GFP and RFP expression. Images were captured with pseudo colored and overlaid using Image J software. *B*, quantification of the relative GFP expression from four independent experiments using two separate reporter construct preparations. Results are shown ± S.D., with a significant difference observed in NHEJ activity between the undamaged or cisplatin-damaged plasmids (*, $p = 0.003$).

and ligation of the linker oligonucleotides (supplemental Fig. S1, *B* and *C*). Two separate preparations each of platinated (Pt+) and unplatinated (Pt−) plasmids were constructed and evaluated for NHEJ efficiency. H460 cells were harvested by trypsinization and co-transfected with circular pCAG-dsRED and either the plasmid containing or devoid of cisplatin end-lesions (Pt+ and Pt−, respectively). As a control, cells were co-transfected with circular pGL1-Mfe1. At 48 h after transfection, the cells were evaluated by fluorescence microscopy. The results presented represent four fields from each well and were quantified in duplicate from four independent experiments. At 200× power, robust GFP expression can be observed in cells transfected with the control circular pGL1-Mfe1 and the non-cisplatin-damaged linear plasmid (Pt−), while significantly reduced GFP expression was observed in the cells transfected with the linear-cisplatin damaged plasmid (Pt+) (Fig. 5*A*). Quantification of the fluorescence microscopic images taken at 80× magnification demonstrates a statistically significant decrease in relative GFP expression in those transfected with the (Pt+) plasmid as compared with those transfected with the (Pt−) plasmid (Fig. 5*B*). These data demonstrate that in the absence of cellular cisplatin treatment, the presence of cisplatin adducts 6-bp from a DNA terminus significantly inhibits the repair of a DNA DSB. Interestingly, there is a low level of GFP expression which could be the result of repair of the cisplatin-damaged DNA, which suggests that the cell may have the ability, albeit significantly reduced, to rejoin a DSB containing a cisplatin lesion. Alternatively, this finding could be attributed, at least in part, to repair of the low level (less than 10%) of undamaged, contaminant plasmid in the (Pt+) preparation.

DISCUSSION

Combination therapy with cisplatin and IR is used routinely for the treatment of many cancers, including NSCLC, and synergy has been observed *in vitro* and *in vivo* in a variety settings (15, 19–21). Although multiple studies have examined the effects of cisplatin on DSB repair, until now, no one has mechanistically separated the downstream signaling effects of cisplatin treatment from the physical presence of cisplatin on the DNA being rejoined. These experiments thus represent the first determination of the downstream effects of cisplatin on NHEJ-catalyzed DSB repair independent of cisplatin lesions on the DNA being rejoined. Additionally, this is the first evidence in live cells that the presence of a cisplatin lesion in close proximity to a DSB impairs NHEJ-catalyzed DSB repair. We show that activation of downstream pathways by cisplatin in cultured NSCLC cells does not significantly affect NHEJ-dependent repair of a DSB on non-cisplatin damaged DNA, but is significantly impaired by the presence of compound cisplatin-DSB lesions in the absence of cellular cisplatin treatment.

Earlier work both *in vitro* and *in vivo* has revealed that cisplatin induced radiosensitization is both time and sequence dependent (4, 20, 21, 30). In addition, while both DSB repair pathways, NHEJ and HR, could potentially impact cisplatin radiosensitization, NHEJ has been demonstrated to be a major determinant of this activity in numerous model systems (15, 18). Cisplatin treatment results in persistent DNA DSBs and has no effect on the repair of IR-induced DNA single-strand breaks (20). Consistent with cisplatin-DNA damage impacting NHEJ, *in vitro* data demonstrate that the presence of cisplatin-DNA lesions resulted in reduced NHEJ activity (15, 18). This is likely a direct result of reduced DNA-PK activity, which our laboratory demonstrated *in vitro* (24, 29). The inhibition of DNA-PK by cisplatin-damaged DNA is spatially related, as cisplatin lesions 6–20 bp from a terminus have been shown to inhibit *in vitro* DNA-PK activity and NHEJ, with more distant cisplatin lesions (60 bp or more) resulting in no significant impairment in DNA-PK activation (15, 23, 25). While these data show a direct effect of cisplatin lesions on the DSB repair process, they do not rule out the possibility that other cisplatin-dependent effects could impact DSB repair. With the formation of 40 DSBs/Gray/cell (31) and cisplatin lesions every 50–500 kb (32), assuming random distribution of damage, the prevalence of a compound cisplatin-DSB lesion would be a rare occurrence. However, there is both experimental and mathematical

data indicating that the combination of IR and cisplatin does not result in the random distribution of damage. *In vitro*, the presence of cisplatin-DNA lesions alters the position of both a bleomycin induced DSB and IR induced DNA damage (33, 34). Extrapolation of these *in vitro* data would suggest that the formation of a DSB in close proximity to a cisplatin-DNA lesion occurs more frequently than by random occurrence and is a physiologically important phenomenon occurring with combined cisplatin-IR treatment. If this is the case, the efficiency of repair of these complex cisplatin-DSB lesions would determine the susceptibility or resistance of cells to combined cisplatin-IR treatment. The presented data suggest that this complex cisplatin-DSB lesion impairs DSB repair, but this would imply that the significantly larger number of cisplatin lesions present on portions of DNA far from a DSB have no impact on DSB repair. The question then arises; is the repair of a DSB without a cisplatin lesion in the vicinity impacted by cisplatin treatment? Any of the downstream effects of cisplatin treatment could be envisioned to impact DSB repair including cell cycle arrest, DNA damage signaling, and initiation of apoptosis. Our results, however, rule out these possibilities and reveal that the major determinant of cisplatin radiosensitization is likely to be a direct effect of a cisplatin lesion on the DNA being rejoined. Taken together, direct inhibition of NHEJ at the site of cisplatin-DNA lesions in close proximity to DNA DSBs is likely to be the cause of the synergistic cytotoxicity seen following combined cisplatin-IR treatment.

While our previous *in vitro* analyses revealed complete inhibition of NHEJ by the presence of a cisplatin lesion in close proximity to a DSB (15), NHEJ activity as quantified by GFP expression in a plasmid containing cisplatin end-lesions is only partially inhibited in an intact cell. There are multiple potential explanations for this observation. The first is that, while rigorous controls were taken in preparing the substrate plasmid, with each step, there remains the possibility of a small, but persistent amount of unplatinated oligonucleotide, undigested pGL1-Mfe1 and unligated linker DNA in the final constructed plasmid. While the byproducts of each steps may be small enough to make *in vitro* detection difficult, they would not require NHEJ (in the case of undigested pGL1-Mfe1) or be devoid of a cisplatin end-lesion, allowing for more efficient NHEJ (in the case of residual unligated or unplatinated plasmid) and would subsequently result in reporter gene expression following transfection of the linear-cisplatin damaged DNA substrate. An alternative explanation is that while the cisplatin lesions severely inhibit NHEJ, a low level of repair occurs in cells that are not observed *in vitro*. Considering the nature of the complex DSB, it is likely that processing of the termini is required for rejoining and could involve Artemis catalyzed nuclease activity and DNA pol λ to prepare the termini for ligation by the DNA ligase IV/XLF/XRCC4 complex. While the *in vitro* NHEJ assay is a robust measure of repair of simple DSBs, it is not clear that the system accurately recapitulates repair of complex lesions and that processing of complex termini in intact cells is considerably more efficient. A third possibility is that an alternative or back-up NHEJ pathway is required to process complex lesions. Alternative NHEJ pathways have been described in a variety of model systems all of which require the deletion or mutation in the factors used for classical NHEJ (35–37). Whether this is truly a novel pathway or the selective use of a subset of proteins is unclear and has been the focus of a recent review (38). While H460 and A549 cells are fully capable of catalyzing classical NHEJ, the potential exists that in the absence of efficient repair via the classical pathway, an alternative pathway is engaged that is less efficient though capable of processing and joining DSBs containing cisplatin lesions. While the amount of repair of the DNA substrate containing the complex lesions is significantly reduced, it has been demonstrated that a single DSB can induce cell death (39). Therefore determination of the proteins and pathways ultimately contributing to the repair of complex cisplatin-DSB lesions holds significant potential to impact the efficacy of combined chemoradiation for cancer treatment.

Acknowledgments—We thank Katherine Pawelczak for design and production of the pGL1-Mfe1 plasmid. We are indebted to all members of the laboratory for helpful discussion and comments regarding this manuscript.

REFERENCES

1. Jemal, A., Bray, F., Center, M. M., Ferlay, J., Ward, E., and Forman, D. (2011) Global cancer statistics. *CA. Cancer J. Clin.* **61,** 69–90
2. Yang, P., Allen, M. S., Aubry, M. C., Wampfler, J. A., Marks, R. S., Edell, E. S., Thibodeau, S., Adjei, A. A., Jett, J., and Deschamps, C. (2005) Clinical features of 5,628 primary lung cancer patients: experience at Mayo Clinic from 1997 to 2003. *Chest* **128,** 452–462
3. Cancer Facts & Figures (2011), *American Cancer Society*, Atlanta
4. O'Rourke, N., Roqué i Figuls, M., Farré Bernadó, N., and Macbeth, F. (2010) *Cochrane Database of Systemic Reviews*, Article No.: CD002140
5. Jett, J. R., Schild, S. E., Keith, R. L., and Kesler, K. A. (2007) Treatment of non-small cell lung cancer, stage IIIB: ACCP evidence-based clinical practice guidelines (2nd Edition). *Chest* **132,** 266S-276S
6. Kartalou, M., and Essigmann, J. M. (2001) Mechanisms of resistance to cisplatin. *Mutat. Res.* **478,** 23–43
7. Siddik, Z. H. (2003) Cisplatin: mode of cytotoxic action and molecular basis of resistance. *Oncogene* **22,** 7265–7279
8. Köberle, B., Grimaldi, K. A., Sunters, A., Hartley, J. A., Kelland, L. R., and Masters, J. R. (1997) DNA repair capacity and cisplatin sensitivity of human testis tumour cells. *Int. J. Cancer* **70,** 551–555
9. Wu, X., Fan, W., Xu, S., and Zhou, Y. (2003) Sensitization to the cytotoxicity of cisplatin by transfection with nucleotide excision repair gene xeroderma pigmentosun group A antisense RNA in human lung adenocarcinoma cells. *Clin. Cancer Res.* **9,** 5874–5879
10. Henkels, K. M., and Turchi, J. J. (1999) Cisplatin-induced apoptosis proceeds by caspase-3-dependent and -independent pathways in cisplatin-resistant and -sensitive human ovarian cancer cell lines. *Cancer Res.* **59,** 3077–3083
11. Tornaletti, S., Patrick, S. M., Turchi, J. J., and Hanawalt, P. C. (2003) Behavior of T7 RNA polymerase and mammalian RNA polymerase II at site-specific cisplatin adducts in the template DNA. *J. Biol. Chem.* **278,** 35791–35797
12. Sorenson, C. M., and Eastman, A. (1988) Mechanism of cis-diamminedichloroplatinum(II)-induced cytotoxicity: role of G2 arrest and DNA double-strand breaks. *Cancer Res.* **48,** 4484–4488
13. Jeggo, P., and Lavin, M. F. (2009) Cellular radiosensitivity: how much better do we understand it? *Int. J. Radiat. Biol.* **85,** 1061–1081
14. Lieber, M. R., Ma, Y., Pannicke, U., and Schwarz, K. (2003) Mechanism and regulation of human non-homologous DNA end-joining. *Nat. Rev. Mol. Cell Biol.* **4,** 712–720
15. Boeckman, H. J., Trego, K. S., and Turchi, J. J. (2005) Cisplatin sensitizes cancer cells to ionizing radiation via inhibition of nonhomologous end

joining. *Mol. Cancer Res.* **3,** 277–285
16. Groen, H. J., Sleijfer, S., Meijer, C., Kampinga, H. H., Konings, A. W., De Vries, E. G., and Mulder, N. H. (1995) Carboplatin- and cisplatin-induced potentiation of moderate-dose radiation cytotoxicity in human lung cancer cell lines. *Br. J. Cancer* **72,** 1406–1411
17. Gorodetsky, R., Levy-Agababa, F., Mou, X., and Vexler, A. M. (1998) Combination of cisplatin and radiation in cell culture: effect of duration of exposure to drug and timing of irradiation. *Int. J. Cancer* **75,** 635–642
18. Myint, W. K., Ng, C., and Raaphorst, G. P. (2002) Examining the non-homologous repair process following cisplatin and radiation treatments. *Int. J. Radiat. Biol.* **78,** 417–424
19. Raaphorst, G. P., Wang, G., Stewart, D., and Ng, C. (1996) Concomitant low dose-rate irradiation and cisplatin treatment in ovarian carcinoma cell lines sensitive and resistant to cisplatin treatment. *Int. J. Radiat. Biol.* **69,** 623–631
20. Dolling, J. A., Boreham, D. R., Brown, D. L., Mitchel, R. E., and Raaphorst, G. P. (1998) Modulation of radiation-induced strand break repair by cisplatin in mammalian cells. *Int. J. Radiat. Biol.* **74,** 61–69
21. Taylor, S. G. 4th, Murthy, A. K., Vannetzel, J. M., Colin, P., Dray, M., Caldarelli, D. D., Shott, S., Vokes, E., Showel, J. L., and Hutchinson, J. C. (1994) Randomized comparison of neoadjuvant cisplatin and fluorouracil infusion followed by radiation versus concomitant treatment in advanced head and neck cancer. *J. Clin. Oncol.* **12,** 385–395
22. Raaphorst, G. P., LeBlanc, J., and Li, L. F. (2005) A comparison of response to cisplatin, radiation and combined treatment for cells deficient in recombination repair pathways. *Anticancer Res.* **25,** 53–58
23. Diggle, C. P., Bentley, J., Knowles, M. A., and Kiltie, A. E. (2005) Inhibition of double-strand break non-homologous end-joining by cisplatin adducts in human cell extracts. *Nucleic Acids Res.* **33,** 2531–2539
24. Pawelczak, K. S., Andrews, B. J., and Turchi, J. J. (2005) Differential activation of DNA-PK based on DNA strand orientation and sequence bias. *Nucleic Acids Res.* **33,** 152–161
25. Turchi, J. J., Henkels, K. M., and Zhou, Y. (2000) Cisplatin-DNA adducts inhibit translocation of the Ku subunits of DNA-PK. *Nucleic Acids Res.* **28,** 4634–4641
26. Patrick, S. M., and Turchi, J. J. (1999) Replication protein A (RPA) binding to duplex cisplatin-damaged DNA is mediated through the generation of single-stranded DNA. *J. Biol. Chem.* **274,** 14972–14978
27. Wood, R. D., Robins, P., and Lindahl, T. (1988) Complementation of the xeroderma pigmentosum DNA repair defect in cell-free extracts. *Cell* **53,** 97–106
28. Baumann, P., and West, S. C. (1998) DNA end-joining catalyzed by human cell-free extracts. *Proc. Natl. Acad. Sci. U.S.A.* **95,** 14066–14070
29. Turchi, J. J., and Henkels, K. (1996) Human Ku autoantigen binds cisplatin-damaged DNA but fails to stimulate human DNA-activated protein kinase. *J. Biol. Chem.* **271,** 13861–13867
30. Aupérin, A., Le Péchoux, C., Rolland, E., Curran, W. J., Furuse, K., Fournel, P., Belderbos, J., Clamon, G., Ulutin, H. C., Paulus, R., Yamanaka, T., Bozonnat, M. C., Uitterhoeve, A., Wang, X., Stewart, L., Arriagada, R., Burdett, S., and Pignon, J. P. (2010) Meta-analysis of concomitant versus sequential radiochemotherapy in locally advanced non-small-cell lung cancer. *J. Clin. Oncol.* **28,** 2181–2190
31. Limoli, C. L., and Ward, J. F. (1995) Photochemical production of double-strand breaks in cellular DNA. *Mutagenesis* **10,** 453–456
32. Parker, R. J., Eastman, A., Bostick-Bruton, F., and Reed, E. (1991) Acquired cisplatin resistance in human ovarian cancer cells is associated with enhanced repair of cisplatin-DNA lesions and reduced drug accumulation. *J. Clin. Invest.* **87,** 772–777
33. Mascharak, P. K., Sugiura, Y., Kuwahara, J., Suzuki, T., and Lippard, S. J. (1983) Alteration and activation of sequence-specific cleavage of DNA by bleomycin in the presence of the antitumor drug cis-diamminedichloroplatinum(II). *Proc. Natl. Acad. Sci. U.S.A.* **80,** 6795–6798
34. Vrána, O., and Brabec, V. (1986) The effect of combined treatment with platinum complexes and ionizing radiation on DNA *in vitro*. *Int. J. Radiat. Biol. Relat. Stud. Phys. Chem. Med.* **50,** 995–1007
35. Corneo, B., Wendland, R. L., Deriano, L., Cui, X., Klein, I. A., Wong, S. Y., Arnal, S., Holub, A. J., Weller, G. R., Pancake, B. A., Shah, S., Brandt, V. L., Meek, K., and Roth, D. B. (2007) Rag mutations reveal robust alternative end joining. *Nature* **449,** 483–486
36. Boboila, C., Yan, C., Wesemann, D. R., Jankovic, M., Wang, J. H., Manis, J., Nussenzweig, A., Nussenzweig, M., and Alt, F. W. (2010) Alternative end-joining catalyzes class switch recombination in the absence of both Ku70 and DNA ligase 4. *J. Exp. Med.* **207,** 417–427
37. Mladenov, E., and Iliakis, G. (2011) Induction and repair of DNA double strand breaks: the increasing spectrum of non-homologous end joining pathways. *Mutat. Res.* **711,** 61–72
38. Neal, J. A., and Meek, K. (2011) Choosing the right path: does DNA-PK help make the decision? *Mutat. Res.* **711,** 73–86
39. Wahl, G. M., Linke, S. P., Paulson, T. G., and Huang, L. C. (1997) Maintaining genetic stability through TP53 mediated checkpoint control. *Cancer Surv.* **29,** 183–219